Quadrupole Centering for CEBAF

T. Satogata
JLAB-TN-14-027

September 25, 2014

This paper describes an algorithm for quadrupole centering in CEBAF, and presents algorithm testing results from elegant simulations. The difference of this algorithm is that it intentionally moves the beam several mm off center in the quadrupole before making quadrupole BDL changes. This improves signal (downstream orbit changes) to noise (BPM noise) for the quadrupole center measurement. It also avoids systematic scaling errors by calculating the quadrupole center from a ratio of two separate position offset measurements.

1 Theory

A beam traveling through a thin quadrupole lens of strength K and length L with transverse position x_q receives an angle kick of

$$x'_{\text{after quad}} - x'_{\text{before quad}} = -(KL)x_q \, . \tag{1.1}$$

If the quadrupole strength changes by ΔK, the change in angle kick from the position offset in the quadrupole is given by

$$\Delta x'_q = -(\Delta K \, L)x_q \, . \tag{1.2}$$

This produces a position change at downstream BPMs from the quadrupole strength change of

$$\Delta x_n = \Delta x'_q \sqrt{\beta_q \beta_n} \sin(\phi_n - \phi_q) = -(\Delta K \, L)x_q \sqrt{\beta_q \beta_n} \sin(\phi_n - \phi_q) \tag{1.3}$$

where $(\beta_{q,n}, \phi_{q,n})$ are the betatron functions and phases at the quadrupole and nth downstream BPM, respectively.

x_q is, however, not directly observable. Assume we have a BPM that is close enough to the quadrupole that its reading x_b can be considered to be the measured position at the quadrupole; this reading includes offset and gain errors from the actual position, where ideally $G_b = 1$ and $x_{b,\text{offset}} = 0$:

$$x_b = G_b x_q + x_{b,\text{offset}} \quad \Rightarrow \quad x_q = \frac{x_b - x_{b,\text{offset}}}{G_b} \tag{1.4}$$

Then (1.3) becomes

$$\Delta x_n = -(\Delta K \, L) \left(\frac{x_b - x_{b,\text{offset}}}{G_b} \right) \sqrt{\beta_q \beta_n} \sin(\phi_n - \phi_q) \tag{1.5}$$

The usual approach to quad steering is to null Δx_n (the motion in downstream BPMs) vs changes in quadrupole strength ΔK by adjusting x_b until $x_b - x_{b,\text{offset}} = 0$. This system is linear, so in an ideal world this process is immediately invertible and $x_{b,\text{offset}}$ in this condition is given by

$$x_{b,\text{offset}} = x_b - \frac{G_b \Delta x_n}{(\Delta K \, L)\sqrt{\beta_q \beta_n} \sin(\phi_n - \phi_q)} \tag{1.6}$$

Note that this solution depends on the BPM gain G_b, the absolute calibration of the change in quadrupole strength ΔK, and the detailed knowledge of the optics transport between the quadrupole and downstream BPM.

We can eliminate those dependencies by performing the measurement at two different BPM positions x_b with the same optics, BPM gain, and quadrupole strength change. For these two measurements, (1.5) becomes

$$\Delta x_{n,1} = -(\Delta K\, L)\left(\frac{x_{b,1} - x_{b,\mathrm{offset}}}{G_b}\right)\sqrt{\beta_q\beta_n}\sin(\phi_n - \phi_q) \tag{1.7}$$

$$\Delta x_{n,2} = -(\Delta K\, L)\left(\frac{x_{b,2} - x_{b,\mathrm{offset}}}{G_b}\right)\sqrt{\beta_q\beta_n}\sin(\phi_n - \phi_q) \tag{1.8}$$

and taking a ratio gives

$$\frac{\Delta x_{n,1}}{\Delta x_{n,2}} = \frac{x_{b,1} - x_{b,\mathrm{offset}}}{x_{b,2} - x_{b,\mathrm{offset}}} \tag{1.9}$$

The cancellation here assumes that G_b and $x_{b,\mathrm{offset}}$ (the gain and offset from the measured BPM position to actual quadrupole position relative to center) are the same for both measurements. This is satisfied if the beam angle at the BPM is unchanged between the two measurements; this steering can be done with a 4-bump (see appendix). The cancellation also assumes that positions are sufficiently small that the relationship between actual and measured BPM position in each BPM is linear.

Solving (1.9) for $x_{b,\mathrm{offset}}$ gives

$$x_{b,\mathrm{offset}} = \frac{x_{b,2}\Delta x_{n,1} - x_{b,1}\Delta x_{n,2}}{(\Delta x_{n,1} - \Delta x_{n,2})} \tag{1.10}$$

This calculation of $x_{b,\mathrm{offset}}$ eliminates most of the systematic error sources from the previous calculation, at the expense of raising the sensitivity to random BPM position measurement noise. That sensitivity can be reduced by taking averages of several BPM position measurements and evaluating (1.10) for many downstream BPMs.

(1.10) can be simplified slightly further by using symmetric initial conditions with $x_b = x_{b,2} = -x_{b,1}$. Then (1.10) becomes

$$x_{b,\mathrm{offset}} = x_b\left(\frac{\Delta x_{n,1} + \Delta x_{n,2}}{\Delta x_{n,1} - \Delta x_{n,2}}\right) \tag{1.11}$$

Both (1.10) and (1.11) can be calculated for each BPM downstream of the quadrupole to give a distribution of measured quadrupole offsets. However, the denominator can be quite small for BPMs that are nearly in phase with the change in transverse kick produced by the quadrupole change, so in practice only offsets calculated for conditions where $\Delta x_{n,1} - \Delta x_{n,2}$ is above a suitable threshold should be included.

A small correction can be applied to the correlation between x_b and x_q when a single upstream corrector is used to adjust the orbit position at the quadrupole/BPM pair. This correction is typically a few percent (about 1.025 on x_b) for a consecutive arc corrector/quadrupole pair such as that in the next section, and comes from the fact that the beam motion in the quadrupole is a systematically different amplitude than that in the nearby BPM. This correction can be avoided by using two upstream correctors as part of a three- or four-bump configuration to change the beam position in the quadrupole as discussed in the appendix, but in practice this is probably a tolerable systematic error for BPM/quadrupole pairs located on the same girder that will be quad centered.

2 Simulations

2.1 Ideal Conditions

Consider a horizontal quad centering of the BPM/quad pair IPM2E02 and MQB2E02, located on the same girder and separated by a distance of 0.45m. MQB2E02 is displaced by $+200\mu$m in the elegant model with the `&alter_elements` command. Adjusting the MBT2E01H corrector by $\pm 0.1893\,\mu$rad moves the orbit by ± 3.0 mm at IPM2E02.

Four beam centroid orbits were generated by an elegant script, simulating four real orbit measurements:

1. The orbit with the MBT2E01H corrector set for +3mm orbit offset at IPM2E02.

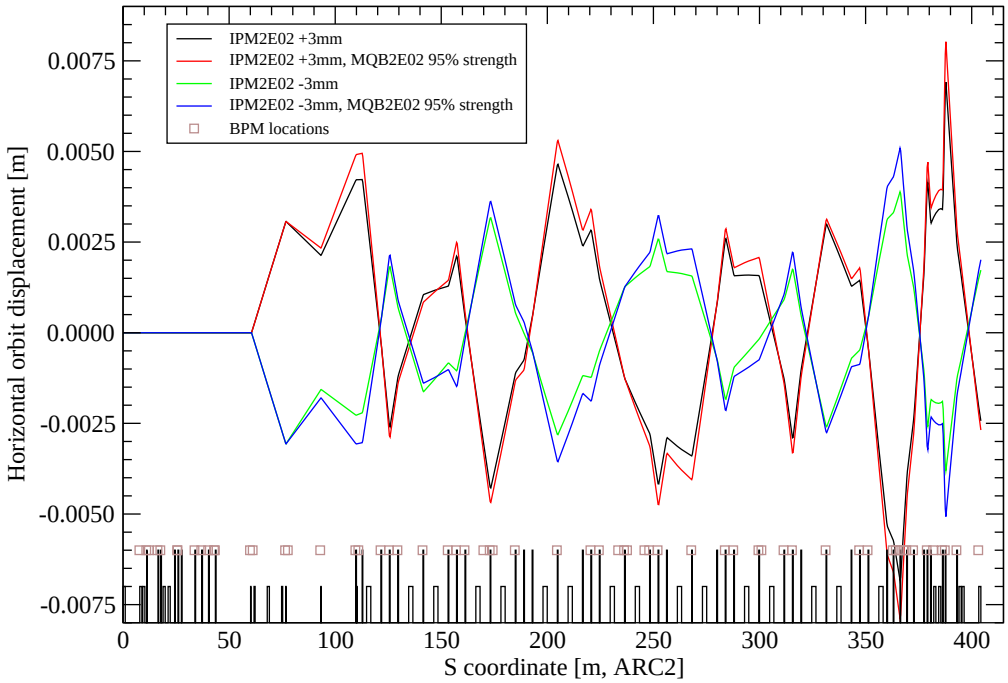

Figure 1: Simulated orbits for horizontal quad centering of MQB2E02 with no BPM noise, and steered orbits of ±3.0 mm at IPM2E02.

2. The orbit with the MBT2E01H corrector set for +3mm orbit offset at IPM2E02, and MQB2E02 lowered in strength by 5%.
3. The orbit with the MBT2E01H corrector set for -3mm orbit offset at IPM2E02.
4. The orbit with the MBT2E01H corrector set for -3mm orbit offset at IPM2E02, and MQB2E02 lowered in strength by 5%.

These orbits are shown in Fig. 1, and the calculated BPM offsets are shown in Fig. 2. The differences in these orbits at each downstream BPM can be used to calculate the quadrupole offset for MQB2E02 using (1.11) with x_b=3.0 mm. With a reasonable denominator cutoff of 500 μm, the simulation exactly reproduces the simulated quadrupole offset.

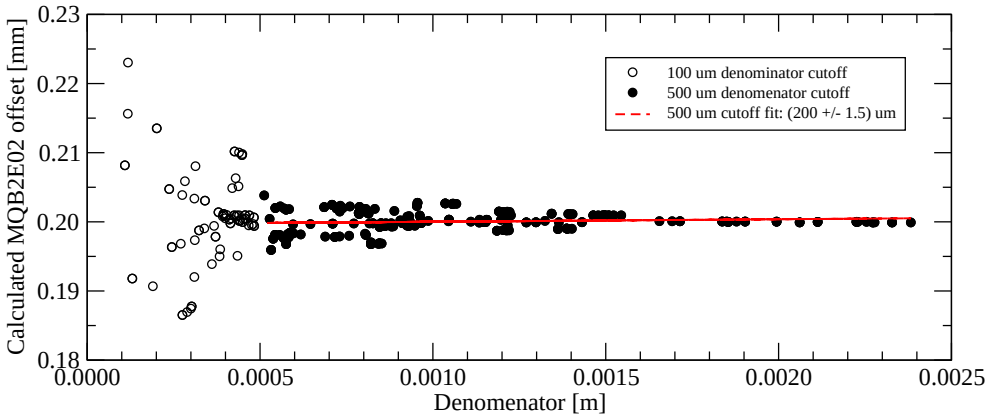

Figure 2: Calculated quadrupole offsets for horizontal quad centering of MQB2E02 with no BPM noise using (1.11) and denominator cutoffs as discussed following (1.11).

2.2 Including BPM Noise

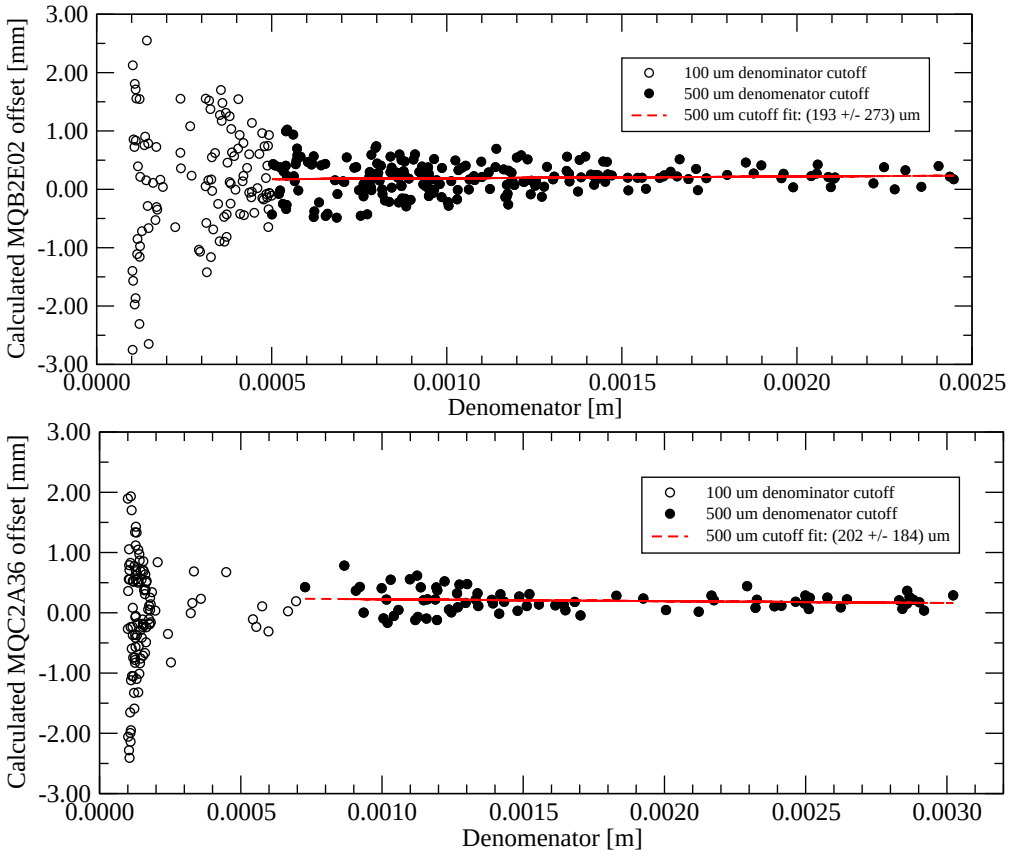

Figure 3: Calculated quadrupole offsets for horizontal quad centering of MQB2E02 and MQC2A36 with uncorrelated 100 μ BPM noise using (11) and denominator cutoffs as discussed following (11).

To evaluate this method's robustness to BPM noise, the simulation above was also run with 100 μm of uncorrelated BPM noise on all BPMs. This is significantly larger noise than expected on CEBAF BPMs, where reasonable averaging is reported to give noise levels of approximately 20 μm, but this is considered to be a worst-case scenario. This corresponds to an attempt to resolve a quadrupole offset (200 μm) that is twice the size of the BPM noise.

The same analysis as the previous section was performed, including denominator cutoffs, and the result is shown in Fig. 3. The quadrupole offsets calculated from each individual downstream BPM are now widely distributed, but the statistical center of the ensemble with the cutoff still measures the quadrupole center at the level of 5%.

Fig. 3 also shows the same simulation repeated for MQC2A36, a late arc quad in ARC2. Many more BPMs fall near zero denominator since they are upstream of the quadrupole and therefore show only a noise response to the quadrupole changes. However, there are still enough BPMs downstream of the quadrupole at high enough response to give a well-resolved offset measurement. A cutoff threshold of 0.5-1 mm seems reasoanable for the analysis with these results.

3 Application

The assumption here is that the BPM positions as reported are

$$\mathrm{XPOS} = \mathrm{XRAW} - (\mathrm{XSOF} + \mathrm{XGOF})\,, \tag{3.12}$$

that XGOF is the general offset used for intentional orbit displacement (e.g. in the arcs to accommodate path length), and that XSOF is the survey offset of the BPM center relative to the nearest quadrupole center that can be adjusted based on quad centering measurements. So only XSOF is modified in the below procedure.

1. Configurable parameters for the quadrupole centering application that should be set before beginning are:
   (a) The quadrupole/BPM pair to be centered and the plane in which they are to be centered. Call these Q_1 and B_1. This can be selected from a CED-generated list of quadrupole/BPM pairs that are both on the same girder and preferably less than 1m apart in s-coordinate, organized by section and s-coordinate. It doesn't matter whether the quadrupole or BPM occurs first in s-coordinate order. Examples of such pairs include IPM1S01/MQB1S01, IPM1E01/MQB1E01, IPM1A01/MQB1A01, and MQB2L01/IPM2L01.
   (b) BPM +/- steering offset x_b (in mm).
   (c) Analysis denominator cutoff (in mm) as described in section 2.2.
2. Identify the in-plane dipole corrector upstream of Q_1 from CED, preferably one girder away. Call this dipole corrector D_1. This corrector will be used to steer the beam at Q_1 and B_1.
3. Fetch CED in-plane beta and phi for D_1 and B_1. and calculate the corrector strength $\Delta x'$ change necessary to move the beam by $+x_b$ at Q_1:
$$\Delta x' = x_b/(\sqrt{\beta_{Q1}\beta_{D1}}\sin\phi_{Q1} - \phi_{D1}) \tag{3.13}$$
4. Check that Q_1, B_1, and D_1 are functional and that Q_1 is on hysteresis. Produce an error if they are not.
5. Cache the SOF value for B_1.
6. User: Ensure that the accelerator is configured for tune beam, typically 4-8 μA, terminated at a dumplette significantly downstream (at least half an arc) of the quadrupole/BPM pair to be centered. This is so the measurement has a reasonable number of downstream BPMs available, while keeping the beam reasonably short. The user should also confirm that the orbit is reasonably well-corrected to the termination point before continuing.
7. Display (or have the user display) the ARC BPM absolute spikes screen for the relevant arc.
8. Construct a list of all BPMs from IPM0L01 to the beam termination point from CED.
9. Start ezlogging `XPOS` and `YPOS` values for all BPMs in the list, the Q_1 BDL, the D_1 BDL, and `IBC0R08CRCUR1.VAL` at a 1 Hz update rate.
10. Pause 10 seconds to acquire baseline orbit data.
11. Change the D_1 BDL as calculated with (3.13) to move the beam by $+x_b$ at B_1.
12. Pause 10 seconds to acquire baseline orbit data with the orbit shifted by $+x_b$ at B_1.
13. Inhibit the beam.
14. Cache the Q_1 BDL setting.
15. Change the Q_1 BDL by 5% of its nominal setting, being careful to stay on hysteresis, and wait for it to settle.
16. Enable the beam.
17. Pause 10 seconds to acquire orbit data with the orbit shifted by $+x_b$ at B_1 and the quad changed.

18. Inhibit the beam.
19. Restore the original Q_1 BDL setting and wait for it to settle.
20. Enable the beam.
21. Repeat steps 9-19, moving the beam by $-x_b$ at B_1.
22. Stop the ezlogger.
23. Data acquisition complete.
24. The fit is the average of the calculations of $x_{b,\mathrm{offset}}$ in Eqn. (1.11) with the denominator larger than the cutoff; the error bar is the RMS of these calculations.
25. Analysis should calculate Eqn. (1.11) for all BPMs downstream of B_1 from ezlogger data, using averages of multiple beam positions where possible, and display a plot of measured responses and fit quad offset measurement as shown in, e.g., Fig. 2.
26. Ask the user to verify the data and quality of fit, and whether the offset should be applied. If they agree that the offset should be applied, calculate $\mathrm{SOF_{new}}$=$\mathrm{SOF_{cached}}$+$x_{b,\mathrm{offset}}$ and set this as the new B_1 SOF for this plane.
27. Procedure complete.

The application should support a batch mode where a user-selected group of BPMs in one section are all measured and set automatically. All settings, cached values, and intermediate calculations should be logged.

---

4 Appendix: Orbit Three-Bump and Four-Bump

4.1 Three-Bump Theory

Some of the algorithms here steer the orbit locally using a three-bump, or a local orbit change made with three dipole correctors. This localizes an intentional orbit change in a single plane at the quadrupole while limiting downstream orbit changes.

Consider three co-planar dipole correctors numbered 1–3 that provide angle kicks

$$\Delta x_i' = \frac{\Delta(BL)_i}{(B\rho)} \tag{4.14}$$

where $(B\rho) = p/|q|$ is the beam rigidity. These dipole correctors have transport matrices between them given by the model, e.g.

$$M(1\to 2) = \begin{pmatrix} M_{11}(1\to 2) & M_{12}(1\to 2) \\ M_{21}(1\to 2) & M_{22}(1\to 2) \end{pmatrix} \tag{4.15}$$

A three-bump is localized if the net orbit change in x and x' from all three corrector kicks $\Delta x_i'$ is zero:

$$M(2\to 3)\left[M(1\to 2)\begin{pmatrix} 0 \\ \Delta x_1' \end{pmatrix} + \begin{pmatrix} 0 \\ \Delta x_2' \end{pmatrix}\right] + \begin{pmatrix} 0 \\ \Delta x_3' \end{pmatrix} = \begin{pmatrix} 0 \\ 0 \end{pmatrix} \tag{4.16}$$

This gives two constraints for three degrees of freedom; the third degree of freedom is constrained by specifying the displacement of the three-bump at the second corrector, Δx_2.

The three corrector kick changes necessary to create a closed bump of amplitude Δx_2 at the second corrector are then

$$\Delta x_1' = \frac{\Delta x_2}{M(1\to 2)_{12}} \tag{4.17}$$

$$\Delta x_2' = -\left[\frac{M(2\to 3)_{11}M(1\to 2)_{12} + M(2\to 3)_{12}M(1\to 2)_{22}}{M(1\to 2)_{12}M(2\to 3)_{12}}\right]\Delta x_2 \tag{4.18}$$

$$\Delta x_3' = \left(\frac{M(2\to 3)_{12}}{(M(1\to 2)_{12})^2}\right)\Delta x_2 \tag{4.19}$$

The corresponding change in control system BDL can then be calculated from (4.14):

$$\Delta(BL)_i = \Delta x_i'(B\rho) \tag{4.20}$$

$$\Delta(BL)_i\,[\mathrm{G-cm}] \approx 3335\,\Delta x_i'\,[\mathrm{rad}]\,p\,[\mathrm{MeV/c}] \tag{4.21}$$

Matrix elements (4.15) used in Eqns (4.17-4.19) for the corrector kicks can be acquired from elegant simulations using the `&matrix_output` command, or can be calculated from CED design optics parameters at the correctors by:

$$M(1\to 2)_{11} = \sqrt{\frac{\beta_2}{\beta_1}}[\cos\Delta\psi + \alpha_1 \sin\Delta\psi] \tag{4.22}$$

$$M(1\to 2)_{12} = \sqrt{\beta_1\beta_2}\,\sin\Delta\psi \tag{4.23}$$

$$M(1\to 2)_{21} = -\frac{[\alpha_2-\alpha_1]\cos\Delta\psi + [1+\alpha_1\alpha_2]\sin\Delta\psi}{\sqrt{\beta_1\beta_2}} \tag{4.24}$$

$$M(1\to 2)_{22} = \sqrt{\frac{\beta_1}{\beta_2}}[\cos\Delta\psi - \alpha_2 \sin\Delta\psi] \tag{4.25}$$

4.2 Three-Bump Example

For example, consider the correctors MBT2E01H, MBT2E02H, and MBT2E03H, which can be used for a three-bump at the MQB2E02 quadrupole. The optics parameters as given by CED for these correctors are:

Parameter	**MBT2E01H**	**MBT2E02H**	**MBT2E03H**
β_x [m]	11.3111	67.6155	8.99423
α_x	-0.7158	3.04035	-0.21590
ψ_x [rad]	4.01080	4.63165	5.39379

The calculated transport matrix elements are given by (4.22-4.25):

$$M(1\to 2)_{11} = 0.97061 \tag{4.26}$$

$$M(1\to 2)_{12} = 16.08772\,\mathrm{m} \tag{4.27}$$

$$M(1\to 2)_{21} = -0.08573\,\mathrm{m}^{-1} \tag{4.28}$$

$$M(1\to 2)_{22} = -0.39071 \tag{4.29}$$

$$M(2\to 3)_{11} = 1.02947 \tag{4.30}$$

$$M(2\to 3)_{12} = 17.02749\,\mathrm{m} \tag{4.31}$$

$$M(2\to 3)_{21} = 0.08589\,\mathrm{m}^{-1} \tag{4.32}$$

$$M(2\to 3)_{22} = 2.39207 \tag{4.33}$$

The corrector kicks are given by (4.17-4.19):

$$\Delta x_1' = (0.06216\,\mathrm{m}^{-1})\,\Delta x_2 \tag{4.34}$$

$$\Delta x_2' = (-0.03617\,\mathrm{m}^{-1})\,\Delta x_2 \tag{4.35}$$

$$\Delta x_3' = (0.06579\,\mathrm{m}^{-1})\,\Delta x_2 \tag{4.36}$$

For a total beam energy (or, very nearly, momentum) in ARC2 of $p = (106.92 + 950.4 + 950.4)\,\mathrm{MeV/c}$ as run late in the spring 2014 run, a bump amplitude of $\Delta x_2 = 3.0\,\mathrm{mm}$ gives the necessary changes in corrector settings of

$$\Delta BDL(\mathrm{MBT2E01H}) = 1248.606\,[\mathrm{G-cm}] \tag{4.37}$$

$$\Delta BDL(\mathrm{MBT2E02H}) = -726.616\,[\mathrm{G-cm}] \tag{4.38}$$

$$\Delta BDL(\mathrm{MBT2E03H}) = 1321.544\,[\mathrm{G-cm}] \tag{4.39}$$

4.3 Four-Bumps

The three-bump described above creates a transverse orbit displacement that is localized to three correctors, but the orbit angle also changes everywhere within the bump. To control angle and position independently, one can use two consecutive overlapping three-bumps that share the same two center correctors. This is known as a four-bump.

If each of the three-bumps has the same orbit displacement, the overall effect of the four-bump is to move the orbit between the centermost two correctors without changing the orbit angle. This can be used, for instance, to move the beam position at the quadrupole for quad centering without changing the beam angle. This can also be used for controlled transverse aperture exploration. This is known as a position four-bump, or a symmetric four-bump since the orbit displacement in each of the three-bumps is the same.

If each of the three-bumps has equal and opposite orbit displacement, the overall effect of the four-bump is to change the orbit at the point midway between the centermost two correctors without changing the orbit position. This is known as an angle four-bump, or an antisymmetric four-bump since the orbit displacement in each of the three-bumps is equal and opposite.

These two four-bump modes (symmetric and anti-symmetric) are independent, so a four-bump can be used to give completely control of beam position and angle independently at the center of the four-bump, while keeping the orbit distortion localized to the region within the four correctors that comprise the bump.